Biosensors and Bioelectronics 176 (2021) 112917

Contents lists available at ScienceDirect

Biosensors and Bioelectronics

journal homepage: http://www.elsevier.com/locate/bios

Short communication

# Electrokinetic sandwich assay and DNA mediated charge amplification for enhanced sensitivity and specificity

Siddharth Sourabh Sahu [a], Christiane Stiller [b], Elizabeth Paz Gomero [b], Ábel Nagy [b], Amelie Eriksson Karlström [b], Jan Linnros [c], Apurba Dev [a,c,*]

[a] Department of Electrical Engineering, The Ångström Laboratory, Uppsala University, Uppsala, Sweden
[b] Department of Protein Science, School of Chemistry, Biotechnology, and Health (CBH), KTH Royal Institute of Technology, Stockholm, Sweden
[c] Department of Applied Physics, School of Engineering Sciences, KTH Royal Institute of Technology, Stockholm, Sweden

ARTICLE INFO

*Keywords:*
Sandwich assay
Label-free detection
DNA-Conjugated affinity probes
Biosensor
Electrokinetics
Streaming current
Zeta potential
Improved specificity and sensitivity

ABSTRACT

An electrical immuno-sandwich assay utilizing an electrokinetic-based streaming current method for signal transduction is proposed. The method records the changes in streaming current, first when a target molecule binds to the capture probes immobilized on the inner surface of a silica micro-capillary, and then when the detection probes interact with the bound target molecules on the surface. The difference in signals in these two steps constitute the response of the assay, which offers better target selectivity and a linear concentration dependent response for a target concentration within the range 0.2–100 nM. The proof of concept is demonstrated by detecting different concentrations of Immunoglobulin G (IgG) in both phosphate buffered saline (PBS) and spiked in *E. coli* cell lysate. A superior target specificity for the sandwich assay compared to the corresponding direct assay is demonstrated along with a limit of detection of 90 pM in PBS. The prospect of improving the detection sensitivity was theoretically analysed, which indicated that the charge contrast between the target and the detection probe plays a crucial role in determining the signal. This aspect was then experimentally validated by modulating the zeta potential of the detection probe by conjugating negatively charged DNA oligonucleotides. The length of the conjugated DNA was varied from 5 to 30 nucleotides, altering the zeta potential of the detection probe from $-9.3 \pm 0.8$ mV to $-20.1 \pm 0.9$ mV. The measurements showed a clear and consistent enhancement of detection signal as a function of DNA lengths. The results presented here conclusively demonstrate the role of electric charge in detection sensitivity as well as the prospect for further improvement. The study therefore is a step forward in developing highly selective and sensitive electrokinetic assays for possible application in clinical investigations.

## 1. Introduction

Electrokinetic methods such as streaming current/potential have been explored for the purpose of bio-recognition because they are sensitive, label-free and inexpensive methods that do not require a large sample volume (Wasilewska and Adamczyk, 2011; Wu et al., 2012). The methods have been utilized for detection of a wide variety of biological targets ranging from antibodies and various other proteins, (Dev et al., 2016), DNA (Li et al., 2018) and extracellular vesicles (Cavallaro et al., 2019) to non-biological targets (Sadlej et al., 2009). The key aspect of these methods is exploiting the changes in the electrostatic and hydrodynamic environment at the solid-liquid interface when target molecules bind to the surface. Like other charge-based sensors, the electrokinetic principles also suffer from Coulomb screening, limiting their application in high salinity buffers (Jaafar et al., 2009). The hydrodynamic influence, on the other hand, offers the benefit to detect particles having insignificant or no charge contrast with the substrate (Adamczyk et al., 2010; Michelmore and Hayes, 2000). Previous theoretical and experimental investigations (Adamczyk et al., 2010; Sadlej et al., 2009; Sahu et al., 2020) have extensively studied electrokinetic phenomena, in particular the hydrodynamic and the electrostatic influence of particle adsorption on the inner surface of a microchannel, revealing a complex dependence of the electrokinetic signals on these parameters. Using a set of engineered molecules and the theoretical model proposed by Adamczyk et al. (2010), we have shown in our previous study (Sahu et al., 2020) that the size and the charge

* Corresponding author. Department of Applied Physics, School of Engineering Sciences, KTH Royal Institute of Technology, Stockholm, Sweden.
*E-mail address:* apurba.dev@angstrom.uu.se (A. Dev).

https://doi.org/10.1016/j.bios.2020.112917
Received 13 October 2020; Received in revised form 27 November 2020; Accepted 17 December 2020
Available online 30 December 2020

parameters of adsorbing particles may either counteract or assist in electrokinetic sensing leading to a very large difference in the limit of detection. The results offer important insight on how to design a sensitive electrokinetic assay. However, for any practical biosensor, the issues of specificity and selectivity are also extremely important. Particularly, in case of immunoassays, it is well-known that the detection of a target molecule often suffers from a low selectivity due to various non-specific interactions and cross-reactivity (Afsahi et al., 2018; Juncker et al., 2014; Lichtenberg et al., 2019; Pei et al., 2013) of the affinity probes with non-target molecules. This is of particular concern when the target is to be detected from a complex medium e.g. plasma or serum. Among the available strategies to mitigate such problems, sandwich immunoassay is widely used in various well-established sensing platforms (Kim and Lee, 2017; Shui et al., 2018; Sun et al., 2019). In this strategy, a target is detected by two affinity probes each directed against different epitopes of the target, and thereby significantly minimizing the responses arising from non-specific and/or cross-reactive interactions with non-target entities. While sandwich assays are an extremely well known and widely used setup for detection of biomolecules, they are usually accompanied by the use of labels (reporter groups) for amplifying the detectable signal (Pei et al., 2013). The labels usually range from enzymes (Tang and Ren, 2008), nano-particles (Su et al., 2010) to fluorescence tags (Cui et al., 2007) conjugated to the detection antibodies and have been mainly validated by various standard methods e.g. surface plasmon resonance (SPR), quartz crystal microbalance, chemi- and electrochemi-luminescence, etc. (Pei et al., 2013). However, the application of sandwich assays in label-free approaches, particularly in electrical sensors, has been very limited.

In this article, we show that an electrical sandwich immunoassay can be realized by using the streaming current method for specific biomolecule detection. The proof of principle is demonstrated by using the immunoglobulin-binding Z-domain, derived from the B domain of staphylococcal protein A, and the therapeutic monoclonal antibody trastuzumab (IgG) as a model affinity pair. In the assay, trastuzumab is used as a target molecule while the Z-domain is used both as capture probe and the detection probe, targeting two binding sites in the Fc region of the antibody. We show that the proposed assay can detect the target both in phosphate buffered saline (PBS) as well as in a complex medium (*E. coli* cell lysate) with a higher specificity compared to the direct assay. Furthermore, by conjugating single-stranded DNA oligonucleotides to the detection probe, we modulated their zeta potential and used them to demonstrate that a better detection sensitivity can be achieved. Experiments performed with various lengths of DNA show that the sensitivity increases with the length of DNA, indicating the influence of the charge of the DNA-conjugated probes. The limit of detection for the sandwich assay as obtained from calibration curves was ~140 pM and ~90 pM for Z-domain and 15 nt DNA-conjugated Z-domain, respectively, demonstrating an increase in sensitivity when using a charge-optimized detection probe.

## 2. Materials

Ultra-pure water was obtained from the Milli-Q synthesis water purification system (Merck Millipore, Germany). Phosphate buffered saline solution (1× PBS) composed of 137 mM NaCl, 2.7 mM KCl and 10 mM phosphate buffer with a pH of 7.4 was obtained from VWR. Microcapillaries made of silica, and with a diameter of 25 μm were obtained from RISE Acreo AB. As model IgG, we used trastuzumab (Herceptin®, Roche). All other chemicals were purchased from Sigma-Aldrich unless stated otherwise.

## 3. Methods

### 3.1. Preparation of DNA-conjugated Z-domain

The unmodified Z-domain was expressed and purified from *E. coli* cultures similarly as published (Altai et al., 2017). The Z-domain was then modified with the three different DNA oligonucleotides via Sortase A-mediated coupling using Sortase A3* (P94S, D196N, K196T), using a previously described protocol (Altai et al., 2017; Stiller et al., 2019). The preparation details of the DNA-conjugated Z-domain along with the sequence of amino acids (Z-domain) and oligonucleotides (DNA-conjugate) used in this study are presented in the supplementary information. Both unmodified Z-domain and Z-DNA-conjugates were diluted to 50 μM in 1× PBS, aliquoted à 20 μL and stored at −20 °C until further use.

### 3.2. Capillary functionalization

The inner surface of each capillary was functionalised using the protocol outlined in our earlier work (Dev et al., 2016). The surface was first cleaned with a TL1 mixture (5:1:1 mixture of Milli-Q water, 30% $H_2O_2$ and 25% $NH_4OH$) at 88 °C for 10 min. This process also activated the hydroxyl groups on the surface for silanisation carried out in the subsequent step, with 5% w/v APTES in 95% ethanol. This was followed by incubation of 1% glutaraldehyde (GA) in 1× PBS solution for 1 h that serves as a linker molecule. Thereafter, a 5 μM solution of Z-domain (the capture probe) was flowed through the capillary for 1 h for its immobilization on the GA surface. The unreacted aldehyde groups were subsequently deactivated by flowing Tris-ethanolamine (0.1 M Tris buffer and 50 mM ethanolamine, pH 9.0) blocking solution for 30 min. To further block non-specific interactions, this was followed by a treatment with 0.05% w/v casein solution for 30 min, for both the capillary surface and the inner walls of all connecting tubes and the hollow Pt electrodes. The capillaries were then stored under nitrogen atmosphere at $+4^0$C until measurement. The length of the capillaries used in the experiments was ~4.5 cm.

### 3.3. Fluidic and electrical measurements

Details about our measurement setup is given in our earlier work (Dev et al., 2016) and are summarized in Fig. 1a. In brief, a commercial Elveflow pressure regulator (OB1) was used for creating periodic pressure pulses in the liquid flowing through the capillary. For the generation of a continuous train of rectangular pulses, the lower value was set at 1.5 bar and the upper value at 3 bar. The flow rate in the capillary was measured via a flow sensor (Elveflow, MSF3). The streaming current ($I_s$) generated as a result of the pressure driven flow was measured using a sensitive sourcemeter (Keithley 2636A) with the help of hollow Pt tube electrodes connected at the inlet and the outlet of the capillary. The measured values of the pressure and streaming current were used to estimate the apparent zeta potential ($\zeta^*$) (Dev et al., 2016). The $\zeta^*$ of the surface was measured by flowing 0.1× PBS buffer, hereafter referred to as baseline measurements. This was done before and after each injection of the sample plug containing target or detection probes. The sample injection was carried out in 1× PBS to better mimic the physiological conditions.

Fig. 1b shows the measurement sequence. Each measurement started with the recoding of the 1st baseline. Thereafter, the target was injected at a fixed applied pressure of 1.5 bar. The rate of target conjugation to the capture probe was monitored by following the changes in $I_s$. As the interaction between the target and the probes is a dynamic one, the injection was carried out until $I_s$ attained an equilibrium value. At this point, the sample injection was replaced by the PBS buffer injection and the 2nd baseline was measured. Switching from sample injection to the measurement buffer drives the dynamic reaction in the reverse direction (dissociation of the target-probe pair). Hence, the duration of the second baseline was fixed to be 20 min for each measurement. This was followed by the injection of the detection probe at a fixed concentration of 200 nM. Finally, the third baseline was measured. This phase involves two overlapping dissociation processes, the target from the capture probe and the detection probe from the target. Therefore, a fixed point

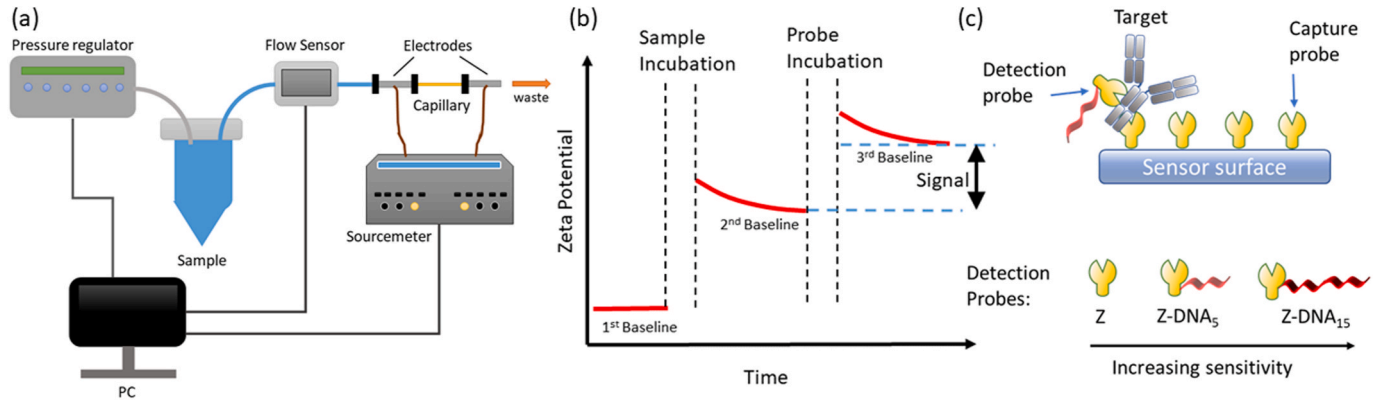


**Fig. 1.** Schematic representation of (a) the experimental setup and (b) the sequence of a multistep measurement for the sandwich assay, starting with the recording of the 1st baseline, followed by the injection of the target until an equilibrium is reached. Thereafter, the 2nd baseline is recorded for a fixed duration. After the injection of the detection probe, the recording of the 3rd baseline follows. The signal of the sandwich assay is the difference indicated by the double-arrow. Panel (c) shows (top) a schematic of a sandwich assay, depicting the target, along with the capture and detection probes (not drawn to scale) and (bottom) the detection probe and its charge modification with the conjugation of DNA oligonucleotide of different lengths.

was chosen at 20 min past the commencement of the 3rd baseline. The signal was calculated as the difference between this point and the end point of the 2nd baseline, as indicated by the double-arrow in Fig. 1b, i.e. the signal, $\Delta\zeta^* = \zeta_f^* - \zeta_i^*$ where $\zeta_f^*$ refers to the zeta potential at the 3rd baseline and $\zeta_i^*$ refers to that of the 2nd baseline.

### 3.4. The model system: two Z-domains as probes binding to the target trastuzumab

For the proof of concept study presented here, we utilized the trastuzumab-Z-domain affinity pair (Fig. 1c, top). The trastuzumab (T) molecule is symmetrical with two identical binding sites for the Z-domain in the Fc region (Ultsch et al., 2017). This offers the benefit of simplicity as the same molecule can be used both as capture and detection probe. The selection was further motivated by the fact that the pair has a reasonably good charge contrast as required for a sensitive electrokinetic assay (Adamczyk et al., 2010; Sahu et al., 2020). At the measurement pH of 7.4, the Z-domain has a negative zeta potential of $-7.1 \pm 0.8$ mV and trastuzumab has a positive zeta potential of $21.4 \pm 0.3$ mV (Table 1). To study the influence of electric charges, the zeta potential of the detection probe was modified by conjugating DNA oligonucleotides of different lengths, hereafter referred to as Z-DNA$_X$, where X represents the number of nucleotides in the conjugated DNA strand (Fig. 1c, bottom). The zeta potential of all the different molecules used in this study (Table 1) was measured by electrophoretic light scattering (details in the supplementary information). As expected, the magnitude of $\zeta_p$ increases with the length of the DNA-conjugate, therefore, validates that the conjugation steps were successful. The purity of the probes was also measured using high performance liquid chromatography (HPLC) and the data are presented in Fig. S2 (supplementary information).

**Table 1**
Details of the targets and probes used along with their $\zeta_p$ measurements using electrophoretic light scattering (ELS).

| Symbol | Protein | Conjugation | $\zeta_p$ (mV) |
|---|---|---|---|
| **T** | Trastuzumab | – | 21.4±0.3 |
| **Z** | Z-domain | – | −7.1±0.8 |
| **Z-DNA$_5$** | Z-domain | 5 nt DNA | −9.3±0.8 |
| **Z-DNA$_{15}$** | Z-domain | 15 nt DNA | −12.9±0.5 |
| **Z-DNA$_{30}$** | Z-domain | 30 nt DNA | −20.1±0.9 |

### 3.5. Measurement of interaction affinity between T and various detection probes

The affinity of different Z-DNA conjugates towards trastuzumab and the kinetics of binding were analysed by SPR-based biosensor experiments using a Biacore 8K system. T was immobilized on a Series S Sensor Chip CM5 (GE Healthcare) with an immobilization level of 2584 RU. See supplementary information for further details. Five different concentrations of the analytes were prepared for the sensorgrams; 80, 40, 20, 10, 5 nM for Z-DNA$_{30}$, 15, 7.5, 3.75, 1.88, 0.94 nM for Z-DNA$_5$, and 42.5, 21.3, 10.6, 5.3, 2.7 nM for Z. The dissociation constant ($K_D$) values were calculated in the Biacore Insight Evaluation software using Langmuir 1:1 binding model.

## 4. Results

Examplary experimental data corresponding to the schematic measurement sequence (Fig. 1b) are presented in Fig. 2a. The surface with immobilized Z-domain as capture probe showed an apparent zeta potential ($\zeta_1^*$) of $-32.5 \pm 0.3$ mV. Upon the binding of the positively charged T molecules (100 nM), the apparent zeta potential ($\zeta_2^*$) became less negative, reaching a value of $-15.1 \pm 0.8$ mV. This step constitutes the signal ($\Delta\zeta^* = \zeta_2^* - \zeta_1^*$) of the direct assay. The third baseline, measured after binding the detection probes to the target, again showed a negative shift of the baseline due to the lowering of $\zeta^*$, i.e. ($\zeta_1^* < \zeta_3^* < \zeta_2^* < 0$). This step constitutes the signal ($\Delta\zeta^* = \zeta_3^* - \zeta_2^*$) of the sandwich assay.

### 4.1. Direct vs sandwich assay using unmodified Z-domain as capture and detection probes

Fig. 2b and c shows the responses, presented in bar plots, obtained for different T concentrations, which were measured using both direct and sandwich assay, respectively, with unmodified Z-domain as the capture and detection probes. In each case, the injection of the target was continued until an equilibrium was reached: 3 h for 200 pM, 2 h for 1 nM, 1 h for 10 nM, 30 min for 100 nM and 15 min for 1 $\mu M$. As seen, the signal was found to increase with the concentration in all cases, before saturating around 100 nM. However, compared to the direct assay, the response of the sandwich assay was opposite and also significantly weaker. For example, while the injection of 1 nM of T results in $8.9 \pm 0.9$ mV signal in case of the direct assay, for the sandwich assay with Z as the detection probe, it is only $-1.2 \pm 0.2$ mV. This might indicate, that the limit of detection for the sandwich assay could be worse in the case of

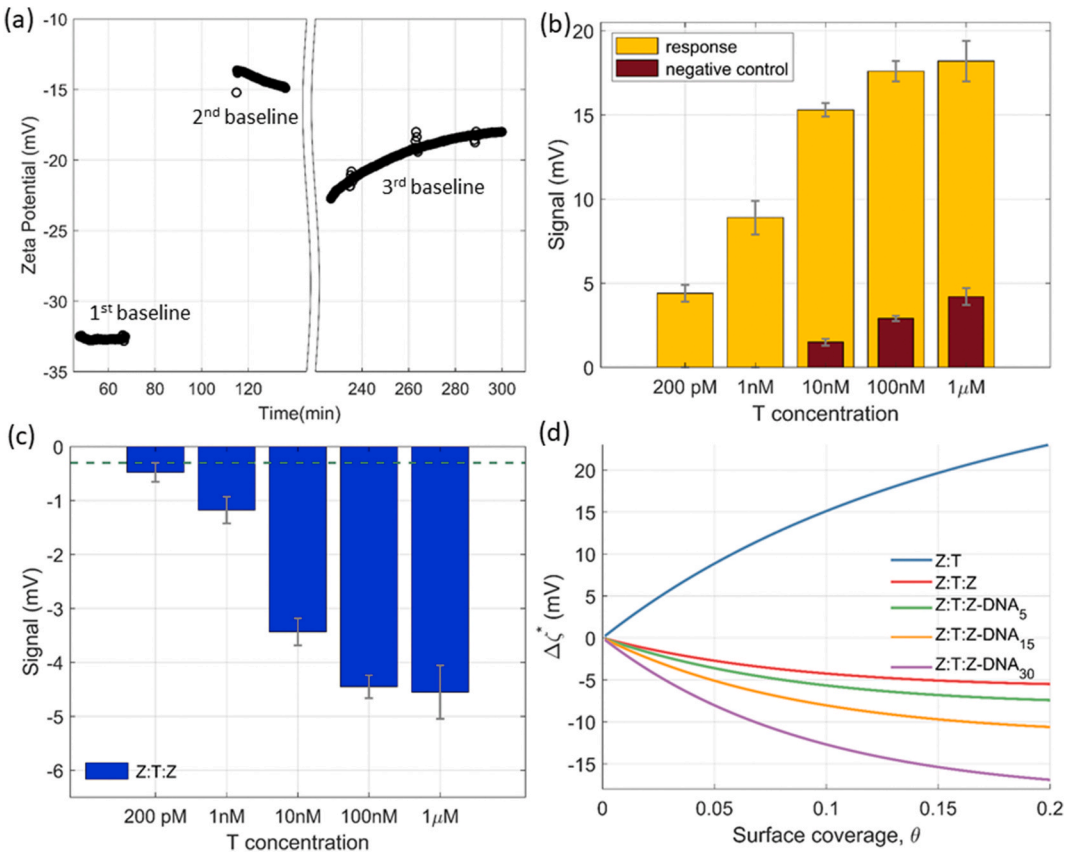


**Fig. 2.** Comparison of the direct and the sandwich assay: panel (a) shows an exemplary experimental data corresponding to the measurement sequence illustrated in Fig. 1b, for 100 nM T. The binding of positively charged target raises the zeta potential in the 2nd baseline, while the binding of the negatively charged detection probe lowers the zeta potential in the 3rd baseline. Moreover, the direct assay response (difference between the 1st and 2nd baselines) is markedly higher than the sandwich assay response (difference between the 2nd and 3rd baselines). Concentration dependent responses obtained from a (b) direct assay and a (c) sandwich assay are shown as bar plots. The negative controls are shown as bar plots in (b) and dotted line in (c). Simulations comparing the signals from the direct assay with the sandwich assay are shown in (d) and demonstrate the possibility of signal enhancement by modulating the charge of the detection probe.

the unmodified Z as detection probe as compared to the direct assay case. However, not only the absolute signal strength, but also the background signal of each assay type needs to be taken into account for a comparison. Therefore, the negative control measurements for each of the assays are also presented as bar plots in Fig. 2b and as a dotted line in Fig. 2c. For the direct assay, the negative control was measured by injecting the target in an identically prepared capillary but without any immobilized capture probes. For the sandwich assay, the negative control measured the interaction between the detection probe and immobilized capture probe, however, without any target molecule (dotted line in Fig. 2c). It can be seen that the negative control for the sandwich assay produces much weaker response in comparison to the direct assay case. The negative control response from the direct assay corresponding to e.g. 100 nM T injection was found to be 1.5 mV which is 17% of the signal for the same concentration. In comparison, the negative controls for the sandwich assay with Z as detection probe only produce 7.3% of the signal for the same concentration of T. As the lower background signal in the sandwich assay only partially counteracts its lower signal strength, we decided to investigate possible improvements for the detection limit of the sandwich assay by altering the zeta potential of the detection probe through conjugation with negatively charged DNA oligonucleotides utilizing theoretical predictions followed by experimental verification.

### 4.2. Simulation results

Simulations were performed to understand if the strong differences in signals, both in magnitude and sign, as obtained from the two different assays, can be explained by the available theoretical models. For this purpose, the model developed by Adamczyk and others (Adamczyk et al., 2010) was used, under some assumptions and approximations (see the supplementary information for details). The same model was previously utilized to explain the effect of molecular size and zeta potential of various targets on the electrokinetic signal (Sahu et al., 2020). According to this model, the signal ($\Delta\zeta^*$) can be expressed in terms of the initial zeta potential ($\zeta_i^*$) of the surface (before the injection of target particle/molecules) and the zeta potential of the injected particles/molecules ($\zeta_p$) by the relation

$$\Delta\zeta^* = -\zeta_i^*\left(1-e^{-C_i\theta}\right)+\zeta_p\left(1-e^{-C_p\theta}\right) \quad (1)$$

The parameters $C_i$ and $C_p$ describe the effect on $\Delta\zeta^*$ induced by the changes in macroscopic flow and electrical charge density, respectively, when target molecules bind to the surface. The fraction of the surface covered by these bound molecules is given by $\theta$. To simulate the response of a direct assay, the value of $\zeta_i^*$ was taken to be the same as the first baseline (−32.5 mV, Fig. 2a), whereas, for the simulation of sandwich assay, the second baseline obtained after 100 nM of T injection (−15.0 mV) was considered. $\zeta_p$ for different molecules used in this study were experimentally measured as presented in Table 1. Fig. 2d presents a set of simulated plots showing the electrokinetic signal as a function of the surface coverage for the two different assays. It is clear that the theoretical model also predicts a strong and positive signal for the direct assay (blue curve) and a significantly weaker and negative response for the sandwich assay (the remaining curves). However, as the zeta potential of the detection probe becomes more negative e.g., when DNA-

conjugated Z is used, the response of the sandwich assay increases. The response continues to increase with increasing length of the DNA.

### 4.3. Effect of zeta potential of the detection probe

To investigate if the charge dependence of the detection probe as predicted by the simulation (Fig. 2d) can be experimentally obtained, we modified the zeta potential of Z by conjugating it with 15 nt long DNA. The response of the sandwich assay for different concentration of T obtained with Z-DNA$_{15}$ as detection probe is presented in Fig. 3a. The Z-DNA$_{15}$ molecules are more negatively charged at the measurement pH condition with a zeta potential of $-9.3 \pm 0.8$ mV compared to Z ($-7.3 \pm 0.8$ mV). A clear signal enhancement was seen when Z-DNA$_{15}$ was used instead of Z as the detection probe. The enhancement was found to be more than 20% for the entire investigated concentration range. The response obtained from a negative control measurement for this case is indicated with a dotted line in Fig. 3a. Calibration curves for the sandwich assays obtained with Z and Z-DNA$_{15}$ as detection probes, respectively, are presented in Fig. S4. The limit of detection (LOD) was estimated to be ~140 pM for Z and ~90 pM for Z-DNA$_{15}$ (details in the supplementary information).

To investigate this charge dependence of the sandwich assay signal even further, we used detection probes with various lengths of DNA conjugated to Z. Fig. 3b shows bar plots of the signal for the sandwich assay when 100 nM of T is used as the target and Z-DNA$_5$, Z-DNA$_{15}$ and Z-DNA$_{30}$ were used as detection probes. It can be seen that the signal proportionally increases when the length of the DNA increases from 5 to 30 nucleotides. The signal obtained with Z-DNA$_{30}$ shows an increase of more than 300% than that obtained with Z-DNA$_5$ for the same target concentration. This clearly indicates the possible influence of a stronger charge contrast between the target and the detection probe. For easier comparison, the signal obtained with Z as detection probe for the same concentration of T is also presented in Fig. 3b. It can be seen that with Z-DNA$_{30}$, the signal roughly doubles than that obtained with Z. However, a comparison of signal obtained with Z and Z-DNA$_5$ shows a clear exception to this pattern where the signal obtained with Z-DNA$_5$ is weaker despite it being more negatively charged compared to Z. It is expected that a difference in affinity between the target and the detection probe due to the presence of DNA oligonucleotides may also produce different responses. To investigate how the conjugation of DNA oligonucleotides to Z alters its affinity to T, the affinity constants of different detection probes used in this study were measured using a commercial SPR system (Biacore 8K, details in the supplementary information). For this purpose, Z, Z-DNA$_5$ and Z-DNA$_{30}$ were used as analytes in a setup where T was immobilized as a ligand on the surface of a CM5 chip and the analytes were allowed to flow over the chip. A representative SPR sensorgram showing the interaction of T and Z for different concentrations of T is presented in Fig. 3c. Similar SPR sensorgrams obtained for the T-Z-DNA$_5$ and T- Z-DNA$_{30}$ interaction pairs are presented in the supplementary material (Fig. S3). The equilibrium dissociation constant ($K_D$) for Z, Z-DNA$_5$ and Z-DNA$_{30}$ were calculated to be 0.89, 1.12 and 3.76 nM, respectively (inset of Fig. 3c). It can be seen that the interaction affinity slightly decreases, i.e. the $K_D$ slightly increases, as DNA oligonucleotides are conjugated to Z. The $K_D$ also increased as the length of the conjugated DNA was increased from 5 nt to 30 nt.

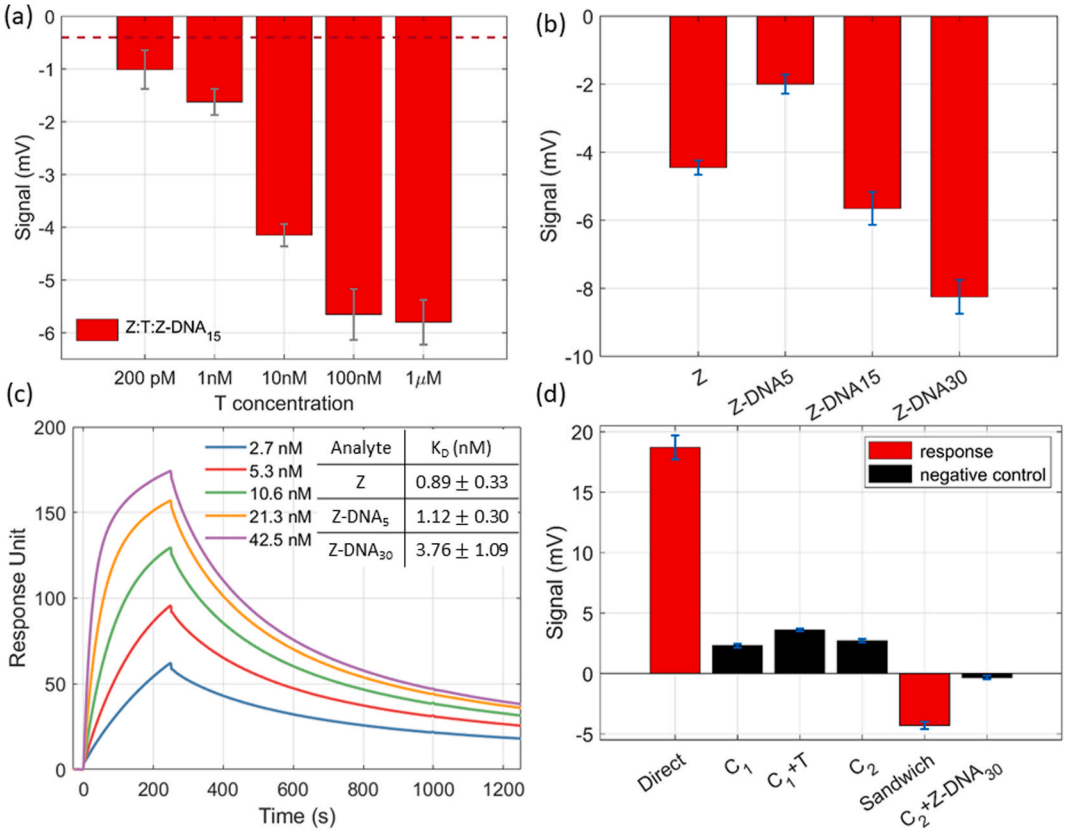


**Fig. 3.** Impact of DNA-conjugation upon the signal: (a) T concentration dependent signal for the sandwich assay step when Z-DNA$_{15}$ is used as the detection probe, with each signal enhanced at least 20% compared to using Z as the detection probe. The negative control is represented by the dotted line. (b) Comparison of the signals when different lengths of the DNA-conjugated Z are used as detection probe for 100 nM T. (c) SPR sensorgram for Z binding to a T surface along with affinity comparison between various detection probes (inset). (d) Response and various negative controls for detection of T from *E. coli* cell lysate diluted 100 times with 1× PBS. Negative controls involved injecting the lysate ($C_1$) and lysate spiked with T ($C_1$+T) on a surface with no immobilized capture probes, and injecting the lysate ($C_2$) and then the detection probe Z-DNA$_{30}$ ($C_2$+Z-DNA$_{30}$) on a surface immobilized with capture probes.

### 4.4. Detection of trastuzumab from a complex medium

As mentioned earlier, one of the major advantages of using a sandwich assay is the increased specificity of detection. To demonstrate this, we performed the detection of the target trastuzumab from a complex medium (Fig. 3d). *E. coli* cell lysate was chosen for this purpose as the bacterial lysate has an abundance of various kinds of proteins (Ishihama et al., 2008). Apart from being a suitable medium to test the specificity of our technique, it has an additional benefit of preventing aggregates from forming (Ishihama et al., 2008). The lysate was diluted 100 times with 1× PBS, mainly to reduce the viscosity. T was then spiked to it so that its final concentration was 100 nM. The response signal and negative controls were recorded for both the direct and sandwich assay steps. The responses as presented in Fig. 3d show a signal of about 18.7 ± 0.9 mV when measured with the direct assay, and a response of only −4.3 ± 0.3 mV when measured with sandwich assay with Z-DNA$_{30}$ as the detection probe. Among the negative controls, $C_1$ involved the capillary functionalization similar to other cases, but with no immobilization of capture probes, followed by the injection of the lysate alone, generating a response of 2.3 mV. When the injection involved spiking T to the lysate ($C_1$ + T), the response was 3.6 mV. Alternatively, injecting the non-spiked lysate over a Z immobilized surface ($C_2$) induced a response of 2.7 mV. However, following the steps in $C_2$ with the injection of Z-DNA$_{30}$ induced the smallest sensor response among all the negative controls: −0.3 mV ($C_2$+ Z-DNA$_{30}$). We define the specificity ratio (SR) as the ratio of the sensor response after target injection to the sensor response after the negative control. With respect to the direct assay step, the SR for $C_1$, $C_1$ + T, and $C_2$ are 5.2, 8.1 and 6.9 respectively. On the other hand, with respect to the sandwich assay step, the SR for $C_2$+ Z-DNA$_{30}$ is 14.3, which is a significant improvement of the SR indicating that this assay type is more specific than the direct assay.

## 5. Discussion

For a sensitive electrokinetic assay, a strong charge contrast between the detection/capture probe and the target molecule is necessary. Given that the probe molecules in our case are smaller in size than the target, the above criterion becomes even more essential in an electrokinetic sandwich assay (Sahu et al., 2020). The influence of molecular charge on the measured signal is clearly visible in Fig. 2a. The surface with immobilized Z was initially negative with an apparent zeta potential of −32.5 mV. When positively charged T bound to the immobilized Z, the surface zeta potential increased. For the measurement of the 2$^{nd}$ baseline, the sample injection was replaced with PBS buffer injection. This is expected to result in a dissociation of the bound T as well as the removal of excess unbound T from the surface leading to a time dependent decrease in the apparent zeta potential, which is visible in the 2$^{nd}$ baseline. This process also happens for the negatively charged detection probe (Z; in the 3$^{rd}$ baseline, resulting in the measured apparent zeta potential drifting towards a more positive value. The influence of molecular charge becomes even more apparent in the results obtained with Z conjugated to DNA oligonucleotides with different lengths (Fig. 3b). This is in good agreement with the simulated results (Fig. 2d). Such a charge dependence of electrokinetic signal has been reported multiple times (Michelmore and Hayes, 2000; Sadlej et al., 2009; Zembala et al., 2001), however, has not been exploited before in an immunoassay. The comparison of interaction affinities for the different probe-target combinations (Fig. 3c) shows that the value of $K_D$ tends to increase as a result of DNA conjugation to Z. Therefore, the increase in sensitivity as observed with Z-DNA$_{15}$ and Z-DNA$_{30}$ as detection probes does not arise due to an increase in affinity. It is rather the opposite i.e. the affinity of Z-DNA$_X$ molecules to T is slightly weaker as compared to Z. The increase of $K_D$ values with the length of the DNA oligonucleotides present on the Z domain suggests that the DNA strand somewhat sterically interferes with the binding of the Z domain to the IgG heavy chain. However, the difference is also not large enough to fully explain the anomalous behaviour that was obtained with Z-DNA$_5$ as detection probe. Nevertheless, the enhancement in signal with Z-DNA$_{15}$ and Z-DNA$_{30}$ despite having weaker affinity to T clearly establishes the proposed principle of signal enhancement by adjusting the charge contrast between target and detection probe. In principle, it could be possible to conjugate a very long DNA strand to the detection probe to further increase the signal, perhaps even exceeding the sensitivity as obtained from the direct assay case. This aspect together with the inconsistent behaviour as obtained with Z-DNA$_5$ as capture probe can be investigated in a follow up study. In addition to molecular charge, the size of molecules also plays an important role. This is evident from the large differences in the signals obtained from the direct and the sandwich assay (Fig. 2b and c). The direct assay shows several times stronger signal than the sandwich assay for all T concentrations studied partly because of the difference in size between T and Z molecule. Estimated hydrodynamic radii of Z and T molecules are 0.6 and 1.5 nm respectively. The influence of molecular size has also been investigated earlier (Sahu et al., 2020) and is mainly attributed to the impedance caused by the molecule to the flow of ions in electric double layer (Adamczyk et al., 2010). This behaviour is also very consistent with the theoretical predictions (Fig. 2d).

The benefit of sandwich assays as compared to direct assays is well-documented (Juncker et al., 2014; Pei et al., 2013). The method is considered to be a gold standard for highly selective detection of a target molecule, particularly from a complex medium containing various other non-target molecules that also possess a certain degree of binding to the same capture probe used for the given target. This is because the probability of two simultaneously spurious bindings is less likely than one such binding (Juncker et al., 2014). A systematic investigation against a panel of various probe-target combinations is normally done to validate a sandwich assay for a given target. This is, however, beyond the scope of the present study. The focus of this work instead is to demonstrate the proof of concept of a label free, electrokinetic sandwich assay that uses electrical means for signal transduction. We do observe however an improvement in SR both when the target medium is clean PBS and when it is the lysate. As presented in Fig. 3d, the sensor response to adsorption/cross reaction of the vast array of proteins present in the lysate is relatively less in the sandwich assay version and the SR improves by several times for the sandwich assay in comparison to the direct assay. On the other hand, the sandwich assay step in case of the lysate shows a signal 48% lower than the case when the medium is purely 1× PBS (Fig. 2d). This is most likely due to the numerous proteins present in the lysate and their non-specific adsorption. The issue of selectivity becomes significantly important as the sensitivity of the sensor and complexity of the sample increases (Wu et al., 2019). For ultra-sensitive biosensors, the chance of false positives is much higher. Hence, finding a compromise between sensitivity and selectivity is imperative for practical application of any sensing technique. The results presented here clearly demonstrate the possibility of improving both the selectivity and the sensitivity of an electrokinetic assay and will certainly facilitate its application in clinical settings.

## 6. Conclusions

In summary, we show a label-free and electrical sandwich immunoassay that uses electrokinetic streaming current method for the signal transduction. The method exploits the charge contrast between the analyte and the detection probe for the generation of sensor response. The proof of principle is demonstrated using IgG as a model analyte and Z-domain as both the capture and the detection probes. The results show a better detection specificity both for simple and complex sample media. Simulations showed a clear prospect for further improvement of the detection sensitivity if the charge contrast between the target and the detection probes can be enhanced. This is then experimentally validated by using DNA-conjugated Z-domain with different lengths of DNA. The results demonstrate that the sensitivity can be increased with increasing length of DNA and the signal enhancement can reach up to ~100% with

just a 30 nt long DNA.

## Credit contribution

Siddharth Sourabh Sahu: investigation, methodology, validation, software, data analysis and visualization, simulations, writing: original draft, review and editing. Elizabeth Paz Gomero: investigation. Christiane Stiller: investigation, methodology, validation, supervision, writing: original draft (protein expression and conjugation), review and editing. Amelie Eriksson Karlström: conceptualization, funding acquisition, project administration, resources, supervision, validation, writing: review and editing. Ábel Nagy: investigation, data analysis and visualization (SPR), writing: original draft (SPR). Jan Linnros: Writing-review & editing. Apurba Dev: conceptualization, supervision, project administration, funding acquisition, resources, validation, writing: original draft, review and editing.

## Declaration of competing interest

The authors declare that they have no known competing financial interests or personal relationships that could have appeared to influence the work reported in this paper.

## Acknowledgments

The authors acknowledge financial support by the Erling Persson foundation. The authors AD and SSS also acknowledge the support from the Swedish Research Council (grant no. 2016–05051).

## Appendix A. Supplementary data

Supplementary data to this article can be found online at https://doi.org/10.1016/j.bios.2020.112917.

## References

Adamczyk, Z., Sadlej, K., Wajnryb, E., Nattich, M., Ekiel-Jezewska, M.L., Bławzdziewicz, J., 2010. Adv. Colloid Interface Sci. 153, 1–29. https://doi.org/10.1016/j.cis.2009.09.004.

Afsahi, S., Lerner, M.B., Goldstein, J.M., Lee, J., Tang, X., Bagarozzi, D.A., Pan, D., Locascio, L., Walker, A., Barron, F., Goldsmith, B.R., 2018. Biosens. Bioelectron. 100, 85–88. https://doi.org/10.1016/j.bios.2017.08.051.

Altai, M., Westerlund, K., Velletta, J., Mitran, B., Honarvar, H., Karlström, A.E., 2017. Nucl. Med. Biol. 54, 1–9. https://doi.org/10.1016/j.nucmedbio.2017.07.003.

Cavallaro, S., Horak, J., Hååg, P., Gupta, D., Stiller, C., Sahu, S.S., Görgens, A., Gatty, H. K., Viktorsson, K., El-Andaloussi, S., Lewensohn, R., Eriksson Karlström, A., Linnros, J., Dev, A., 2019. ACS Sensors acssensors. https://doi.org/10.1021/acssensors.9b00418, 9b00418.

Cui, R., Pan, H.C., Zhu, J.J., Chen, H.Y., 2007. Anal. Chem. 79, 8494–8501. https://doi.org/10.1021/ac070923d.

Dev, A., Horak, J., Kaiser, A., Yuan, X., Perols, A., Björk, P., Karlström, A.E., Kleimann, P., Linnros, J., 2016. Biosens. Bioelectron. 82, 55–63. https://doi.org/10.1016/j.bios.2016.03.060.

Ishihama, Y., Schmidt, T., Rappsilber, J., Mann, M., Harlt, F.U., Kerner, M.J., Frishman, D., 2008. BMC Genomics 9, 1–17. https://doi.org/10.1186/1471-2164-9-102.

Jaafar, M.Z., Vinogradov, J., Jackson, M.D., 2009. Geophys. Res. Lett. 36, L21306. https://doi.org/10.1029/2009GL040549.

Juncker, D., Bergeron, S., Laforte, V., Li, H., 2014. Curr. Opin. Chem. Biol. 18, 29–37. https://doi.org/10.1016/j.cbpa.2013.11.012.

Kim, S., Lee, H.J., 2017. Anal. Chem. 89, 6624–6630. https://doi.org/10.1021/acs.analchem.7b00779.

Li, Y., Lai, S.N., Zheng, B., 2018. Sensors Actuators B Chem 259, 871–877. https://doi.org/10.1016/J.SNB.2017.12.130.

Lichtenberg, J.Y., Ling, Y., Kim, S., 2019. Sensors (Switzerland). https://doi.org/10.3390/s19112488.

Michelmore, A.P., Hayes, R.A., 2000. PhysChemComm. https://doi.org/10.1039/b001277g, 3.

Pei, X., Zhang, B., Tang, J., Liu, B., Lai, W., Tang, D., 2013. Anal. Chim. Acta 758, 1–18. https://doi.org/10.1016/j.aca.2012.10.060.

Sadlej, K., Wajnryb, E., Bawzdziewicz, J., Ekiel-Jeewska, M.L., Adamczyk, Z., 2009. J. Chem. Phys. 130 https://doi.org/10.1063/1.3103545.

Sahu, S.S., Stiller, C., Cavallaro, S., Karlström, A.E., Linnros, J., Dev, A., 2020. Biosens. Bioelectron. 152 https://doi.org/10.1016/j.bios.2020.112005.

Shui, B., Tao, D., Cheng, J., Mei, Y., Jaffrezic-Renault, N., Guo, Z., 2018. Analyst 143, 3549–3554. https://doi.org/10.1039/c8an00527c.

Stiller, C., Aghelpasand, H., Frick, T., Westerlund, K., Ahmadian, A., Eriksson Karlström, A., 2019. Bioconjugate Chem. 30, 2790–2798. https://doi.org/10.1021/acs.bioconjchem.9b00548, 2019.

Su, B., Tang, J., Chen, H., Huang, J., Chen, G., Tang, D., 2010. Anal. Methods 2, 1702–1709. https://doi.org/10.1039/c0ay00468e.

Sun, D., Lu, J., Zhang, L., Chen, Z., 2019. Anal. Chim. Acta 1082, 1–17. https://doi.org/10.1016/j.aca.2019.07.054.

Tang, D., Ren, J., 2008. Anal. Chem. 80, 8064–8070. https://doi.org/10.1021/ac801091j.

Ultsch, M., Braisted, A., Maun, H.R., Eigenbrot, C., 2017. Protein Eng. Des. Sel. 30, 619–625. https://doi.org/10.1093/protein/gzx029.

Wasilewska, M., Adamczyk, Z., 2011. Langmuir 27, 686–696. https://doi.org/10.1021/la102931a.

Wu, J., Zhang, Y., Zhao, L., Zou, L., Alvarez, J.C., Pu, Q., 2012. Sensors Actuators, B Chem. 174, 18–23. https://doi.org/10.1016/j.snb.2012.08.013.

Wu, Y., Tilley, R.D., Gooding, J.J., 2019. J. Am. Chem. Soc. 141, 1162–1170. https://doi.org/10.1021/jacs.8b09397.

Zembala, M., Adamczyk, Z., Warszyski, P., 2001. Colloids Surfaces A Physicochem. Eng. Asp. 195, 3–15. https://doi.org/10.1016/S0927-7757(01)00825-1.